

Lecture 7: Passive Ocean Models

7.1 Preliminaries

The most conspicuous roles of the ocean in climate are storage and transport of energy. Less obvious perhaps are storage and transport of properties such as freshwater or salt; nutrients; carbon; chemical tracers. The *storage* role of the ocean can be characterised as *passive*, whereas the *transport* role is *active*, since it involves ocean dynamics. While arguably the transport side is more interesting, certainly to oceanographers, the storage role has some important aspects as well, some of which we will explore in this lecture.

The ocean has a vastly larger heat capacity than the atmosphere. Ten metres of water weigh as much as the entire atmosphere (ocean density, ρ_O , is 10^3 times atmospheric surface density, ρ_A ; the atmospheric mass can be represented in a 10 km thick layer of air with roughly surface density – the “scale height”, H_A). The heat capacity per unit mass, $c_{p,O}$, of the ocean is 4 times that of the atmosphere, $c_{p,A}$. Hence, *2.5 metres of water hold as much heat as the entire atmosphere*. The mixed layer (surface part of the ocean that is continuously well mixed and in contact with the atmosphere) is typically 50m deep (giving 20 times the heat capacity of the atmosphere); the deep ocean is 5000m deep (2000 times the capacity of the atmosphere).

Numbers for heat capacity per unit area are:

Atmosphere:

$$C_A = c_{p,A} \rho_A H_A = 10^3 \text{Ws kg}^{-1} \text{K}^{-1} \times 1 \text{kg m}^{-3} \times 10 \times 10^3 \text{m} = 10^7 \text{Ws m}^{-2} \text{K}^{-1} \quad (7.1)$$

Ocean (mixed layer):

$$C_O = c_{p,O} \rho_O H_O = 4 \times 10^3 \text{Ws kg}^{-1} \text{K}^{-1} \times 10^3 \text{kg m}^{-3} \times 50 \text{m} = 2 \times 10^8 \text{Ws m}^{-2} \text{K}^{-1} \quad (7.2)$$

Thermal equilibration timescales are:

Atmosphere: Two months ($C_A / B \approx 10^7 \text{Ws m}^{-2} \text{K}^{-1} / 2 \text{W m}^{-2} \text{K}^{-1} \approx 5 \times 10^6 \text{s} \approx 50 \text{days}$), using a longwave coefficient, B, from the energy balance models

Mixed layer: Two months

($C_o / \lambda \approx 2 \times 10^8 \text{ W s m}^{-2} \text{ K}^{-1} / 35 \text{ W m}^{-2} \text{ K}^{-1} \approx 6 \times 10^6 \text{ s} \approx 60 \text{ days}$), the choice of air-sea interaction coefficient, λ , is nontrivial; we will return to it later.

Deep ocean: 1000 years ($H^2 / k_v \approx 4 \times 10^6 \text{ m}^2 / 10^{-4} \text{ m}^2 \text{ s}^{-1} \approx 4 \times 10^{10} \text{ s} \approx 1300 \text{ years}$), with deep-ocean depth scale H and vertical diffusivity k_v .

Exercise:

1. Derive the scaling for the deep-ocean adjustment time. Hint: Estimate the magnitude of the terms in the vertical diffusion equation, $\partial T / \partial t = k_v \partial^2 T / \partial z^2$.

The most familiar consequence of the ocean's large heat capacity is the smaller seasonal cycle in maritime climates, compared to continental climates. Here, we wish to explore the consequences of coupling an inert, long-memory medium (the ocean) to a fast medium, the atmosphere. The ocean is passive in that it is merely a reservoir, albeit a finite one. While mixed layer depth could change as a consequence of the interaction with the atmosphere, we will not consider this here. We will, however, investigate in some detail two highly non-trivial consequences that arise from the ocean's large heat capacity – adjustment to equilibrium in an energy balance model (EBM), and climate variability induced by random forcing.

7.2 Finite heat capacity and response time in energy balance models

To derive the adjustment timescale in a globally averaged (zero-dimensional, 0-D) EBM, we remember that the change in global heat content (all variables represent global averages) is

$$C \frac{dT}{dt} = \frac{S}{4} (1 - \alpha) - I, \quad (7.3)$$

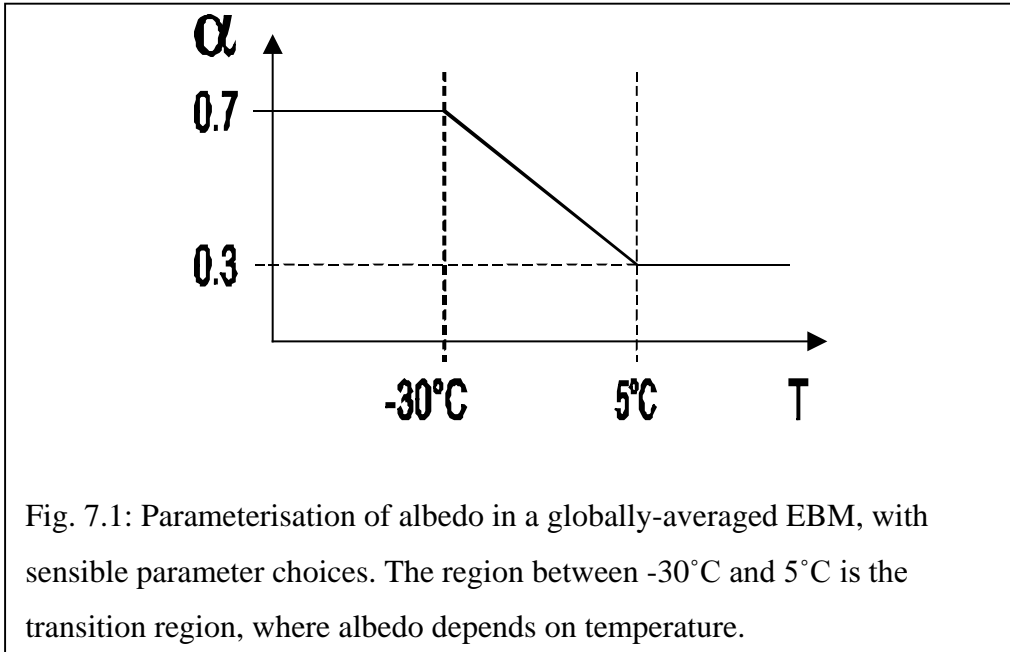
where C is heat capacity, T surface temperature, S total solar output (the quantity formerly known as solar constant – not appropriate since it varies in time), and for longwave radiation I ,

$$I = A + BT. \quad (7.4)$$

The albedo α in the “transition region” (the nontrivial parameter regime where α depends on temperature) is written as

$$\alpha(T) = \alpha_0 - \gamma T; \quad -30 \leq T \leq 5. \quad (7.5)$$

For temperatures above and below the threshold values characterising absence of ice and complete ice cover, respectively, the albedo is constant (see Fig. 7.1).



We define climate sensitivity, β , as the change in global steady-state temperature per fractional change in total solar output (NB: definition is closely related to but different from the one used in Simple Climate Models I)

$$\beta \equiv S \frac{d\bar{T}}{dS}, \quad (7.6)$$

where the overbar marks an equilibrium value. In other words,

$$\Delta\bar{T} \approx \beta \frac{\Delta S}{S} \quad (7.7)$$

For the model defined through the energy conservation equation, (7.3), the steady-state condition is

$$\bar{T} = \frac{S}{4}(1 - \bar{\alpha}), \quad (7.8)$$

for which it is readily shown that

$$\beta \equiv S \frac{d\bar{T}}{dS} = \frac{\bar{T}}{B - \gamma S/4}. \quad (7.9)$$

[Derivation of (7.9): Differentiation on both sides with respect to S of the steady-state energy

balance, (7.8), gives

$$\frac{d\bar{I}}{d\bar{T}} \frac{d\bar{T}}{dS} = \frac{1}{4}(1-\bar{\alpha}) - \frac{S}{4} \frac{d\bar{\alpha}}{d\bar{T}} \frac{d\bar{T}}{dS} \quad (7.10)$$

or

$$\frac{d\bar{T}}{dS} \left[\frac{d\bar{I}}{d\bar{T}} + \frac{S}{4} \frac{d\bar{\alpha}}{d\bar{T}} \right] = \frac{1}{4}(1-\bar{\alpha}) \quad (7.11)$$

Using the parameterisations (7.4) for longwave radiation and (7.5) for the temperature dependence of albedo, and steady-state energy balance (7.8), results in

$$\frac{d\bar{T}}{dS} (B - \gamma S/4) = \frac{1}{4}(1-\bar{\alpha}) = \frac{\bar{I}}{S}, \quad (7.12)$$

or

$$S \frac{d\bar{T}}{dS} = \frac{\bar{I}}{B - \gamma S/4}. \quad \text{q.e.d.} \quad (7.13)$$

To obtain the time-dependent behaviour, assume an initial condition, $T(0)$, not in equilibrium, and write

$$T(t) = \bar{T} + T'(t), \quad (7.14)$$

to obtain, by inserting (7.14) into the energy balance equation (7.3) and using the temperature dependence of albedo, (7.5),

$$C \frac{d}{dt} (\bar{T} + T') = \frac{S}{4} [1 - \alpha_0 + \gamma(\bar{T} + T')] - (A + B\bar{T} + BT'), \quad (7.15)$$

or

$$C \frac{d}{dt} T' = \frac{S}{4} [1 - \alpha_0 + \gamma\bar{T}] - (A + B\bar{T}) + \frac{S}{4} \gamma T' - BT'. \quad (7.16)$$

The first two terms on the right-hand side represent the steady-state energy balance and cancel each other, cf. (7.8). Subtracting the steady-state part from (7.16) therefore yields

$$C \frac{dT'}{dt} = -(B - \gamma S/4) T', \quad (7.17)$$

or

$$\frac{C\beta}{\bar{I}} \frac{dT'}{dt} = -T'. \quad (7.18)$$

N.B.: Equation (7.17) shows explicitly that the steady state is stable (coefficient on right-hand side less than zero) if $B > \gamma S/4$, that is, the negative feedback (longwave radiation) is stronger than positive feedback (ice-albedo).

The solution to (7.17) is

$$T'(t) = T'(0)e^{-t/\tau}, \quad (7.19)$$

where the adjustment time, τ , is

$$\tau \equiv \frac{C\beta}{\bar{I}} = \frac{C}{B - \gamma S/4}, \quad (7.20)$$

proportional both to the heat capacity and to the climate sensitivity. The former is obvious, the latter perhaps less so. To fully appreciate this result, let us look at a concrete initial-value problem, where the total solar output is suddenly increased. We have

$$\begin{aligned} t < 0: \quad S &= S_0; \quad T = \bar{T} = \text{const.} \\ t \geq 0: \quad S &= S_0 + \Delta S; \quad T = \bar{T} + T'; \quad T'(0) = 0 \end{aligned} \quad (7.21)$$

The governing equation is the same as (7.15) but with $S_0 + \Delta S$ replacing S . We assume that ΔS is small compared to S , so that we can neglect higher-order contributions (terms involving products of T' and ΔS). Subtracting the steady-state terms, as before, results in

$$C \frac{dT'}{dt} + (B - \gamma S/4)T' = \frac{\Delta S}{4}(1 - \alpha) = \frac{\Delta S}{S} \bar{I}, \quad (7.22)$$

the latter equality again arising by virtue of the steady-state energy balance, (7.8).

Rewriting (7.22) gives, using the result (7.20) for adjustment timescale,

$$\frac{dT'}{dt} + \frac{T'}{\tau} = \frac{\Delta S}{S} \frac{\beta}{\tau}, \quad (7.23)$$

which has the solution

$$T'(t) = \frac{\Delta S}{S} \beta (1 - e^{-t/\tau}). \quad (7.24)$$

Note that indeed, $T'(0) = 0$. For very long times, the solution goes toward $\beta \Delta S/S$, as it must from the definition of climate sensitivity. For $t \ll \tau$, one obtains, using

$$e^{-t/\tau} \approx 1 - t/\tau$$

$$T'(t) \approx \frac{\Delta S}{S} \frac{\beta}{\tau} t = \frac{\Delta S}{S} \frac{\bar{I}}{C} t, \quad (7.25)$$

where again the result (7.20) for the adjustment timescale has been used. For times shorter than the adjustment timescale, that is, before the net negative feedback kicks in, the temperature increases linearly with time, as if no feedback at all were present. This is equivalent to leaving out the second term on the left-hand side of (7.23). During this linear increase, *the time evolution is independent of the climate sensitivity*. Conversely, it is impossible to infer the climate sensitivity from the early evolution. This is possible only after time longer than τ has passed. Large climate sensitivity means weak negative net feedback and long adjustment timescale [defined as the time when feedbacks become active; see (7.20)].

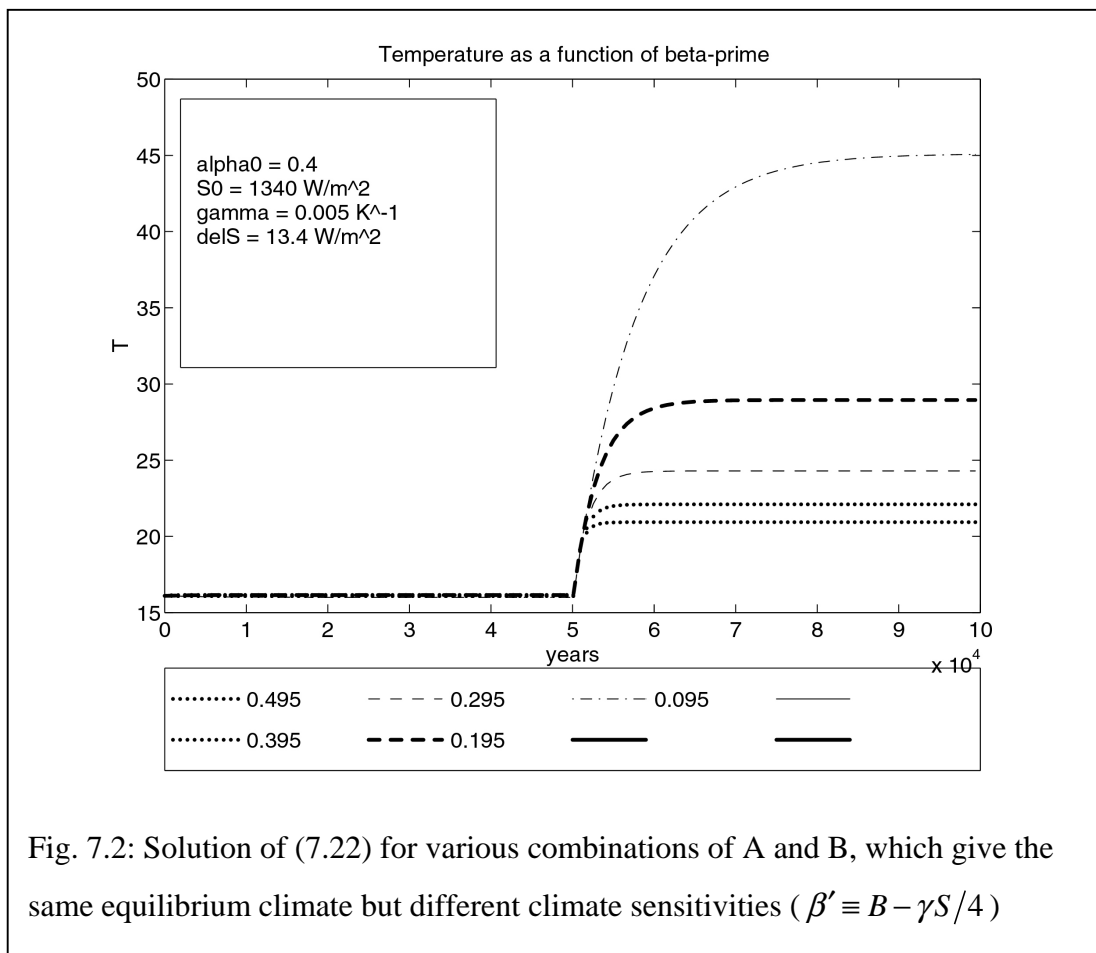


Fig. 7.2: Solution of (7.22) for various combinations of A and B, which give the same equilibrium climate but different climate sensitivities ($\beta' \equiv B - \gamma S/4$)

The short-term response is independent of the climate sensitivity, but it does depend on the heat capacity. The adjustment timescale depends on both, whereas the steady-state temperature response is independent of heat capacity. For transient future climate change, the question is what heat capacity is appropriate, that of the surface

ocean, the thermocline, or the deep ocean? The answer depends on the pathways of heat into the ocean and is very complex.

7.3 Climate variability: stochastic climate models

Up to now, we considered largely steady-state models or the response to a steady (or slow) perturbation. Now we look at climate variability. Hasselmann (1976) introduced the concept of stochastic climate models. He postulated that one could distinguish between two timescales in the climate system, one defining weather (here, the atmosphere; rapid fluctuations), the other defining climate (here, the ocean; slow response). Instead of treating the actual nonlinear interactions between frequency regimes explicitly, we consider “weather” as a *stochastic forcing of climate*.

If, symbolically, “x” denotes weather and “y” denotes climate, we can write

$$\frac{d}{dt} \begin{pmatrix} x \\ y \end{pmatrix} = \begin{pmatrix} N_x(x, y) \\ N_y(x, y) \end{pmatrix}. \quad (7.26)$$

Because of nonlinearities, $N_y \neq N_y(y)$, that is, climate evolution is not solely governed by the climate state but depends on weather. Consequently, climate is not a dynamical system, as stressed by Ed Lorenz (pers. comm.). But we are interested only in climate. Instead of trying a closure (parameterisation of weather effects on climate purely in terms of climate variables), we write

$$\frac{dy}{dt} = -\alpha y + f, \quad (7.27)$$

where f is white noise and where we have assumed the simplest possible “climate dynamics” (linear damping). Concerning weather-climate interactions, we have replaced the nonlinear, chaotic description with a linear, stochastic one. This replacement is also known as a Langevin model or a fluctuation-dissipation approach.

Pedagogical example: The Game of Peter and Paul (after Wunsch (1992)).

A true coin is tossed; if the coin shows heads, Peter pays Paul 1\$; if it shows tails, Paul pays Peter. Figure 7.3 shows Paul’s net earnings as a function of time, first for 50,000, then for 500,000 tosses (executed on the computer, of course). Counter to

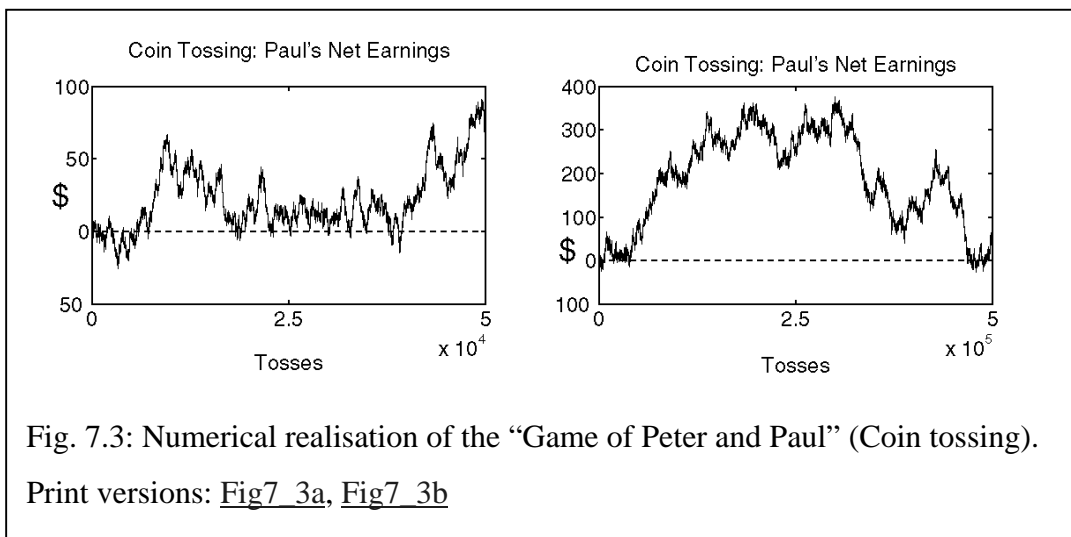


Fig. 7.3: Numerical realisation of the “Game of Peter and Paul” (Coin tossing).

Print versions: [Fig7_3a](#), [Fig7_3b](#)

expectation, which would have the net earnings hover around zero for most of the time, there are large fluctuations away from the break-even point, and one player or the other is far ahead for most of the time. This result may well have a bearing on the real world; the observations by Schott et al. (1988) of mass transport through the Florida Strait (Fig. 7.4) show some similarity to the coin tossing time series.

What is going on? Why does our intuition fail us so profoundly in predicting the outcome of “Peter and Paul”? First, the game shown in Fig. 3 is indeed a fair one; Paul is ahead for much of the time not because of a flaw in the execution of the game but because of an *inevitable* (as we will show) random succession of tosses in his favour. To gain insight, let us first consider a slightly more general case. Write

$$y(t) = \sum_{t'=1}^{t'} \xi(t'), \quad (7.28)$$

where t' takes integer values and ξ is a random process with vanishing ensemble mean, $\langle \xi(t) \rangle = 0$. Notice that the ensemble mean is taken over all possible outcomes, at any given time. Moreover, ξ is “white” (uncorrelated in time) and has variance σ^2 , that is, $\langle \xi(t) \xi(t') \rangle = \sigma^2 \delta_{tt'}$. Here, $\delta_{tt'}$ is the Kronecker delta, with the value of zero if $t \neq t'$ and the value of one if $t = t'$.

Equation (7.28) reflects the summation of a sequence of random events; in the special case of $\xi=1$ or $\xi=-1$, we recover “Peter and Paul”, with total number of coin tosses of t . Writing (7.28) once again but for $t-1$ tosses shows that $y(t)$ is the solution of the very simple difference equation,

$$y(t) = y(t-1) + \xi(t), \quad (7.29)$$

the special case ($a=1$) of a “first-order autoregressive process”, abbreviated AR(1):

$$y(t) = ay(t-1) + \xi(t); \quad 0 \leq a \leq 1. \quad (7.30)$$

For simplicity (and to be fair to both Peter and Paul), we assume that $y(0) = 0$. We see that, if $a > 0$ (that is, the state at a previous timestep matters) $y(t)$ has a “memory”.

Since

$$y(t-1) = ay(t-2) + \xi(t-1), \quad (7.31)$$

$$y(t) = a^2 y(t-2) + a\xi(t-1) + \xi(t), \quad (7.32)$$

we can guess that

$$y(t) = \sum_{t'=1}^t a^{t-t'} \xi(t') = \sum_{t''=0}^{t-1} a^{t''} \xi(t-t''). \quad (7.33)$$

This shows that “old” $\xi(t)$ are eventually “forgotten”, if $a < 1$.

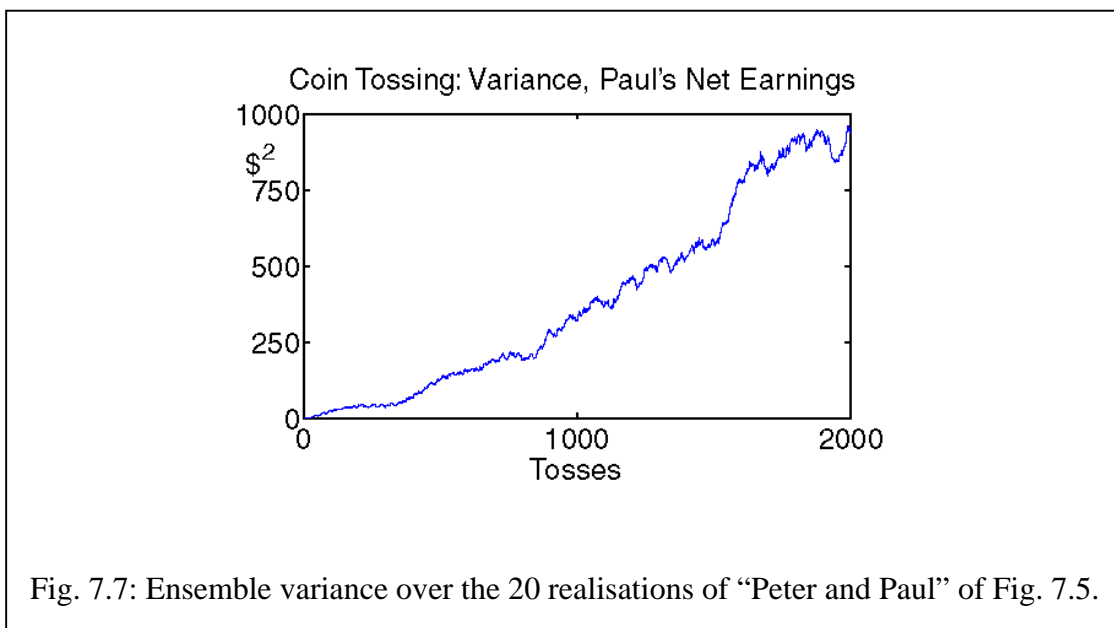
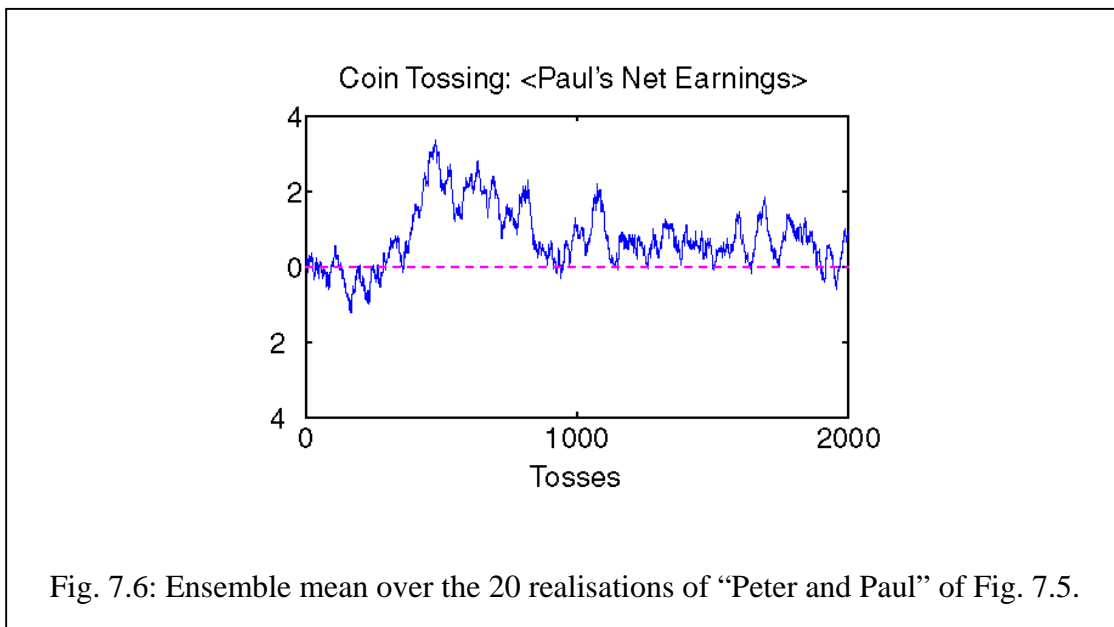
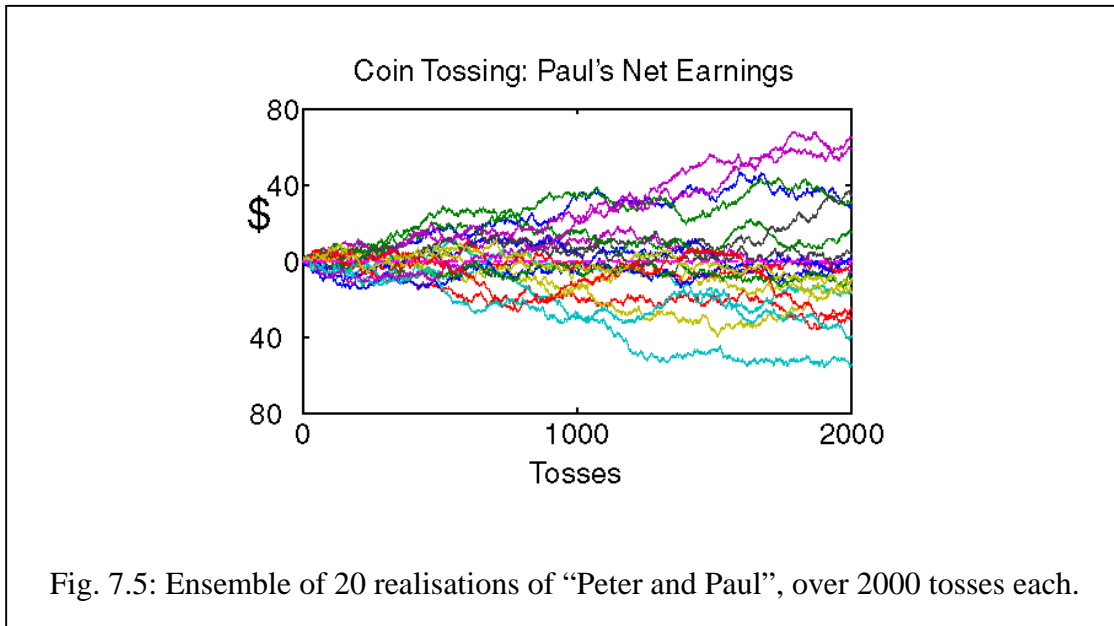
[Proof of (7.33): Insert into difference equations

$$\begin{aligned} y(t) - ay(t-1) &= \sum_{t'=1}^t a^{t-t'} \xi(t') - a \sum_{t'=1}^{t-1} a^{t-1-t'} \xi(t') \\ &= \sum_{t'=1}^t a^{t-t'} \xi(t') - \sum_{t'=1}^{t-1} a^{t-t'} \xi(t') = \xi(t). \quad q.e.d. \end{aligned} \quad (7.34)]$$

We now consider some important statistical properties of $y(t)$. First, the mean (expectation value) of any player’s (here: Paul’s) earnings is given as

$$\langle y(t) \rangle = \sum_{t'=1}^{t-t} a^{t-t'} \langle \xi(t') \rangle = 0, \text{ vanishing mean.} \quad (7.35)$$

This shows that indeed no one player has any advantage in the game, although in the particular outcome shown in Fig. 7.3b Paul seemed so privileged. Figure 7.5 confirms this point empirically. Shown are 20 realisations over 2000 tosses each. Sometimes Paul comes out ahead in the end, sometimes Peter does; over many games, no player wins. Figure 7.6 shows the average over the empirical ensemble in Fig. 7.5; over 20 realisations, no player is ahead by more than about \$3, a trivial amount. However, if we are asking by how far *one player or the other* is ahead, the situation is different. Figure 7.7 shows the variance of Paul’s earnings; the variance counts positive and



negative deviations from the expected value equally. It appears as if the square of Paul's deviation from the break-even point grows by an amount roughly proportional to the number of tosses, consistent with the ever wider spread of the curves in Fig. 7.5.

Theoretically, the variance comes out as

$$\begin{aligned}
 \langle y(t) y(t) \rangle &= \left\langle \sum_{t'=1}^{t'=t} a^{t-t'} \xi(t') \sum_{t''=1}^{t''=t} a^{t-t''} \xi(t'') \right\rangle \\
 &= \sum_{t'=1}^{t'=t} \sum_{t''=1}^{t''=t} a^{t-t'} a^{t-t''} \langle \xi(t') \xi(t'') \rangle \\
 &= \sum_{t'=1}^{t'=t} \sum_{t''=1}^{t''=t} a^{t-t'} a^{t-t''} \sigma^2 \delta_{t',t''} \\
 &= \sigma^2 \sum_{t'=1}^{t'=t} a^{2(t-t')} = \sigma^2 \sum_{\tau=0}^{\tau=t-1} a^{2\tau} \\
 &= \begin{cases} \sigma^2 \frac{1-a^{2t}}{1-a} \xrightarrow{t \rightarrow \infty} \frac{\sigma^2}{1-a}; & a < 1 \\ \sigma^2 t; & a = 1 \end{cases}
 \end{aligned} \tag{7.36}$$

For perfect memory, $a=1$, as in the Game of Peter and Paul (no one loses money except to the other), the variance grows out of bounds, as t goes to infinity. Since $y(t)$ represents Paul's net earnings, this means that the amount by which one player leads, is expected to grow as the square root of time. As they both play with finite resources, sooner or later one must go bankrupt. This result is mathematically equivalent to the analysis of random walk first performed by G.I. Taylor in 1921.

If $a < 1$, meaning there is less than perfect memory, the variance of $y(t)$ about its mean, zero, goes toward a constant, which is larger as a is closer to unity. The damping checks the growth of the variance. Still, the variance of y is greater than that of ξ , owing to the finite memory. It is thus not true that the presence of a "slow" component reduces variability, on the contrary, it increases variability.

As an aside, it does not help to average over $y(t)$ to get rid of the unbounded growth of variance. Define the sample mean over N timesteps,

$$\bar{y}_N \equiv \frac{1}{N} \sum_{t=0}^N y(t), \tag{7.37}$$

the variance of which about the mean can be shown to grow linearly with N:

$$\langle \bar{y}_N^2 \rangle \xrightarrow{N \rightarrow \infty} \sigma^2 \frac{N}{3}. \quad (7.38)$$

Exercises:

2. Show that for the AR(1) process defined by (7.30), nonvanishing memory ($a > 0$) means that the solution $y(t)$ is correlated in time.
3. Prove (7.38). N.B.: Wunsch (1992) has the factor $N/2$, which is not borne out by checks by countless students.

Now, we turn to the low-frequency variability of $y(t)$, clearly shown by the power spectrum, which is “red” (more power at low frequencies, Fig. 7.8), typical of geophysical spectra. The power spectral density is proportional to ω^{-2} , as can be shown by first rewriting the difference equation (7.30) as

$$y(t) - y(t-1) = -(1-a)y(t-1) + \xi(t). \quad (7.39)$$

which plausibly approximates the differential equation

$$\dot{y}(t) = -(1-a)y(t) + \xi(t) \equiv -\kappa y(t) + \xi(t), \quad (7.40)$$

provided that the damping parameter, κ , is much less than unity (damping small over one timestep). Notice that in a continuum formulation, noise can never be truly white, but we will ignore this complication. We will take the Fourier transform, defined by

$$y(t) = \int_{-\infty}^{\infty} \hat{y}(\omega) e^{-i\omega t} d\omega. \quad (7.41)$$

The Fourier transform of white noise (the Dirac delta-function) is a constant, c . The Fourier transform of (7.40) is

$$-i\omega \hat{y}(\omega) = -\kappa \hat{y}(\omega) + c, \quad (7.42)$$

yielding

$$\hat{y}(\omega) = \frac{c}{\kappa - i\omega}. \quad (7.43)$$

We are interested in the real part of the solution; most conveniently we calculate the square of the modulus,

$$|\hat{y}(\omega)|^2 = \frac{c^2}{\kappa^2 + \omega^2} \left\{ \begin{array}{l} \xrightarrow[\kappa \rightarrow 0]{a \rightarrow 1} \frac{c^2}{\omega^2} \\ \xrightarrow{\omega \rightarrow 0} \frac{c^2}{\kappa^2} \\ \xrightarrow{\omega^2 \gg \kappa^2} \frac{c^2}{\omega^2} \end{array} \right. \quad (7.44)$$

The completely undamped system has a power spectrum proportional to ω^{-2} , again confirmed by the numerical example from the coin tossing (Fig. 7.8). With finite damping, the high-frequency part of the spectrum falls off as ω^{-2} , while the low-frequency part tends toward a constant, which is dependent on the damping.

We will not go into further detail, but notice that the appropriate “null-hypothesis” for explaining low-frequency variability in an oceanographic record (e.g., Rockall Channel time series, Fig. 7.9, which is Fig. 12 from Dickson et al. (1988) is forcing by quasi-random atmospheric perturbations. It might be vain to search for a deterministic cause. This lesson is often hard to swallow, because it is sometimes perceived that identification of a specific cause represents a higher level of understanding. But Figs. 7.10 and 7.11, which are Figs. 5 and 6 of Mikolajewicz and Maier-Reimer (1990), clearly show that nontrivial large-scale behaviour can be caused by random surface forcing. Figure 7.11 also shows examples of the theoretical spectrum, (7.44), for various choices of damping. The stochastic theory of climate of Hasselmann (1976) has thus proven to be a very important paradigm for explaining climate variability.

References

- Dickson, R. R., J. Meincke, S.-A. Malmberg, and A. J. Lee, 1988: The "Great Salinity Anomaly" in the northern North Atlantic 1968-1982. *Prog. Oceanogr.*, **20**, 103-151.
- Hasselmann, K., 1976: Stochastic climate models. Part I: Theory. *Tellus*, **28**, 473-485.
- Mikolajewicz, U., and E. Maier-Reimer, 1990: Internal secular variability in an ocean general circulation model. *Clim. Dyn.*, **4**, 145-156.
- Schott, F., T. N. Lee, and R. Zantopp, 1988: Variability of structure and transport of the Florida Current in the period range of days to seasonal. *J. Phys. Oceanogr.*, **18**, 1209-1230.
- Wunsch, C., 1992: Decade-to-century changes in the ocean circulation. *Oceanography*, **5**, 99-106.